Int. J. Radiation Oncology Biol. Phys., Vol. 79, No. 1, pp. 289–296, 2011

0360-3016/$–see front matter

doi:10.1016/j.ijrobp.2010.01.047

PHYSICS CONTRIBUTION

DIGITAL TOMOSYNTHESIS FOR RESPIRATORY GATED LIVER TREATMENT: CLINICAL FEASIBILITY FOR DAILY IMAGE GUIDANCE

Q. Jackie Wu, Ph.D., Jeffrey Meyer, M.D., Jessica Fuller, M.S., Devon Godfrey, Ph.D., Zhiheng Wang, Ph.D., Junan Zhang, Ph.D., and Fang-Fang Yin, Ph.D.

Department of Radiation Oncology, Duke University Medical Center, Durham, NC

Purpose: Breath-hold (BH) treatment minimizes internal target volumes (ITV) when treating sites prone to motion. Digital tomosynthesis (DTS) imaging has advantages over cone-beam CT (CBCT) for BH imaging: BH-DTS scan can be completed during a single breath-hold, whereas BH-CBCT is usually acquired by parsing the gantry rotation into multiple BH segments. This study evaluates the localization accuracy of DTS for BH treatment of liver tumors.

Methods: Both planning CT and on-board DTS/CBCT images were acquired under BH, using the planning CT BH window as reference. Onboard imaging data sets included two independent DTS orientations (coronal and sagittal), and CBCT images. Soft tissue target positioning was measured by each imaging modality and translated into couch shifts. Performance of the two DTS orientations was evaluated by comparing target positioning with the CBCT benchmark, determined by two observers.

Results: Image data sets were collected from thirty-eight treatment fractions (14 patients). Mean differences between the two DTS methods and the CBCT method were <1 mm in all directions (except the lateral direction with sagittal-DTS: 1.2 mm); the standard deviation was in the range of 2.1–3.5 mm for all techniques. The Pearson correlation showed good interobserver agreement for the coronal-DTS (0.72–0.78). The interobserver agreement for the sagittal-DTS was good for the in-plane directions (0.70–0.82), but poor in the out-of-plane direction (lateral, 0.26).

Conclusions: BH-DTS may be a simpler alternative to BH-CBCT for onboard soft tissue localization of the liver, although the precision of DTS localization appears to be somewhat lower because of the presence of subtle out-of-plane blur. © 2011 Elsevier Inc.

Digital tomosynthesis, Image guidance, Respiratory motion, Breath hold, liver.

INTRODUCTION

One of the challenges in irradiating sites such as the liver is organ motion. Studies have shown that liver motion associated with breathing can be several centimeters (1–5). To minimize the motion, treatment using abdominal compression, under deep inspiration breath-hold (BH) or active breathing control (ABC) has been used (6–16). These motion-management techniques can reduce large planning target volumes required to account for liver motion, allowing higher doses to be delivered without increasing normal liver toxicity (9, 17).

The reproducibility of organ position using ABC or BH has been studied for lung and liver cancer patients (7, 10, 11, 18). Dawson *et al.* (7) reported 2.5-mm intrafraction reproducibility and 4.4-mm interfraction reproducibility of liver position relative to the vertebral bodies for six patients using daily orthogonal kilovoltage (kV) imaging. Eccles *et al.* (18) reported the interfraction reproducibility ranges from 1.5 to 7.7 mm in the superior–inferior direction, with average difference of diaphragm positions relative to vertebral body position per patient in the range of 0.1–12.0 mm. Kimura *et al.* (11) also found that the BH reproducibility was 4.0 ± 3.5 mm (intrafraction) and 5.1 ± 4.8 mm at the end-inspiration phase (interfraction). Similarly, Kim *et al.* (10) found the standard deviation of diaphragmatic position for BH ranged from 0.13 to 2.57 mm, with an average of 0.97 mm. These findings indicate a change in diaphragm position from day to day despite using ABC or BH in the same planned position. Therefore, quick daily imaging is preferred to verify target position before treatment (6, 17, 19).

For ABC or deep-inspiration BH treatment, the ideal localization imaging technology should have fast acquisition (*i.e.,* within about 20 s or single BH equivalent) and provide sufficient three-dimensional (3D) visualization of soft tissues.

Reprint requests to: Q. Jackie Wu, Ph.D., Box 3295, Department of Radiation Oncology, Duke University Medical Center, Durham, NC 27710. Tel: (919) 681-1841; Fax: (919) 681-7183; E-mail: Jackie.Wu@duke.edu

The research is in part supported by research grants from National Institutes of Health (Grant No. R21 CA128368), General Electric Medical Systems, and Varian Medical Systems.

Conflict of interest: none.

Received May 14, 2009, and in revised form Jan 29, 2010. Accepted for publication Jan 31, 2010.

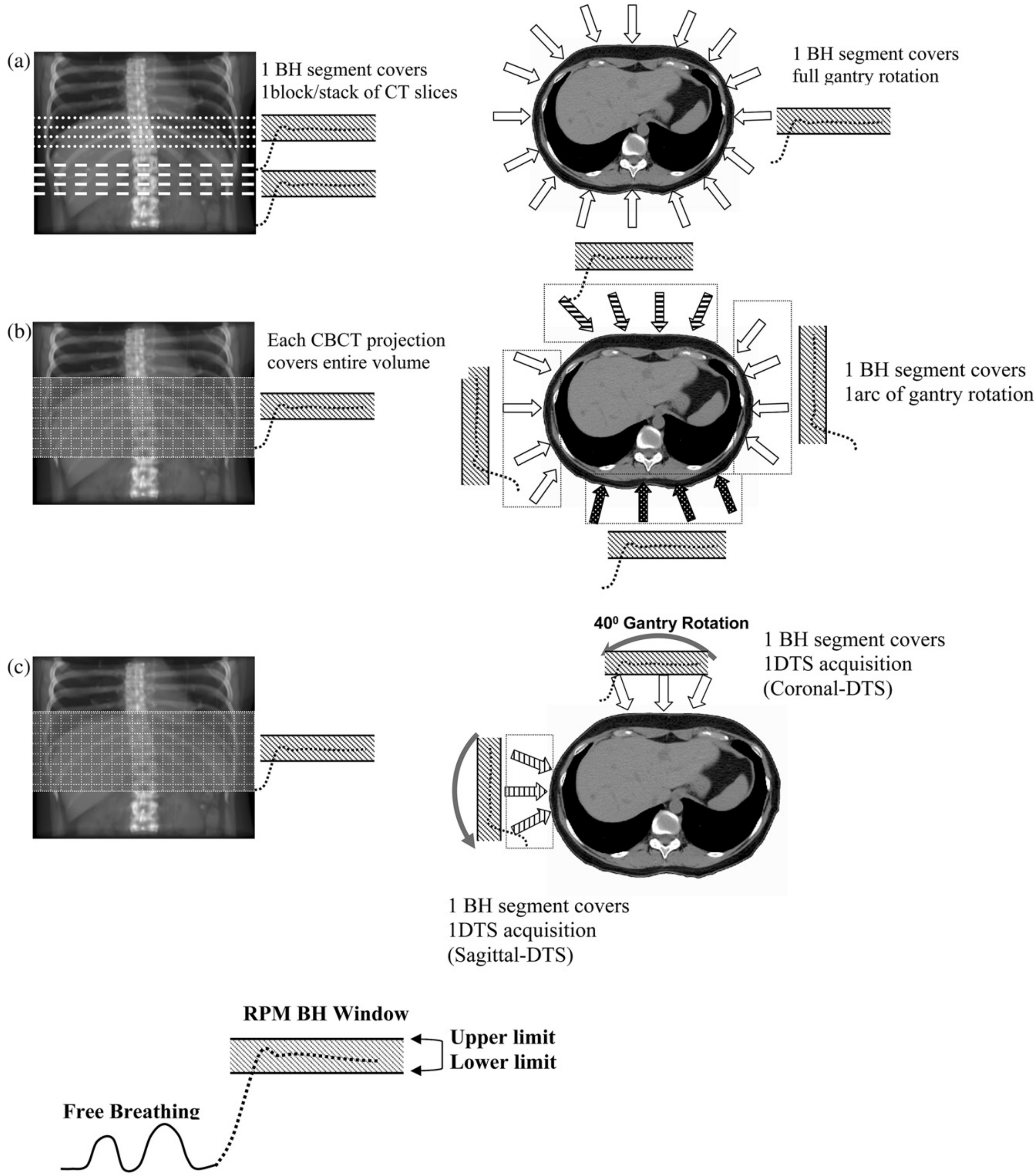

Fig. 1. Distribution of the multiple breath-hold (BH) segments over the imaging acquisition geometry. The BH window is monitored via the respiration monitoring (RPM) system (Varian Medical Systems, Palo Alto, CA) and is shown separately. The shadowed boxes indicate the RPM BH windows that are used to monitor each BH level. The reference BH windows were set at CT simulation and used for all treatment and imaging. During each BH session, it is required that the BH signal remains within the predetermined upper and lower limits. (a) CT geometry. One BH segment allows the scan of 1 block/stack of CT slices. Each BH segment covers a subset of CT slices, and multiple BH segments are distributed in the superior to inferior direction. (b) CBCT geometry. Each BH segment covers a subset of projection images or gantry rotations. Each projection images the entire scan volume. Multiple BH segments are distributed along the gantry rotation direction. (c) Digital tomosynthesis (DTS) geometry (coronal and sagittal). Only a single BH is needed for one BH-DTS acquisition. Each projection images the entire scan volume. Multiple BH segments are required to obtain different DTS views and orientations. The coronal-DTS and sagittal-DTS shown in the figure are considered two independent DTS imaging data sets.

Two-dimensional radiography provides sufficient bony information but lacks soft tissue contrast. Breath-hold cone-beam CT (BH-CBCT) yields good 3D anatomy visibility and soft-tissue contrast (20, 21), but the entire scan must be parsed into multiple BH segments and usually takes 3–5 min. Digital tomosynthesis (DTS) is an alternative 3D imaging technique that yields a stack of slice images acquired with only limited gantry rotation angles (*e.g.,* 40° gantry rotation or 80 X-ray projections) (22). Clinical feasibility of DTS as a 3D imaging guidance tool has been demonstrated in recent studies for head-and-neck treatment (23) and prostate treatment (24). BH digital tomosynthesis (BH-DTS) is an imaging technique ideally suited for this application. BH-DTS has the potential to provide high-quality image information that is comparable to BH-CBCT, and it can be completed in a single patient BH (a typical 40° DTS scan can be acquired in <10 s), making rapid BH-DTS a simpler method for acquiring motion-free 3D localization images than BH-CBCT.

This study analyzes and compares the target localization accuracy between onboard DTS technology and state-of-the-art 3D CBCT technology for BH treatment of liver lesions. The secondary aim of this study was to compare the interobserver variation for DTS and CBCT images.

METHODS AND MATERIALS

Image data

This study included 38 fractions of 14 patients treated with BH external radiation therapy or stereotactic body radiation therapy to the liver. This study was conducted under a protocol approved by the institution's internal review board. To be eligible for BH treatment, patients were required to be able to hold their breath for at least 20 s. Both treatment planning CT and onboard CBCT images were acquired under BH. DTS images were reconstructed using subsets of the CBCT projection data. Details about the imaging acquisition and reconstruction for planning CT, onboard CBCT, and onboard DTS are presented and discussed in the Appendix. Also, the synchronization of BH segments and tomographic projections of different imaging modalities is illustrated in Fig. 1 and described in the Appendix. The CBCT imaging geometries using so-called full fan and half-fan are presented in Fig. 2, and their impact on BH-CBCT/DTS imaging is presented in the Appendix and Fig. 3.

In this study, all the CBCT projections were acquired in the half-fan mode. When operating in the half-fan mode, only half of the anatomy is imaged at one time. Therefore, it takes a full 360° gantry rotation to capture the entire anatomy for CBCT reconstruction. The images are then pieced or stitched together to display a large field-of-view CBCT image. Because the DTS images were reconstructed retrospectively from clinical half-fan CBCT scans, our analysis was performed using two opposed 40° DTS arcs that were stitched together to give the field of view that would otherwise be expected from a single DTS scan, if performed prospectively without the half-fan detector offset. For example, the 20° Right and 20° degree left DTS scans were combined to complete the sagittal view DTS shown in Fig. 3b. This results in a single longitudinal line of discontinuity in the sagittal DTS image, as shown in Fig. 3b, because the two halves of the reconstructed volume are reconstructed from two opposed BH scans. It should be noted that this artifact is simply a result of the study design and would not be present in an actual prospective DTS scan performed with a centered detector.

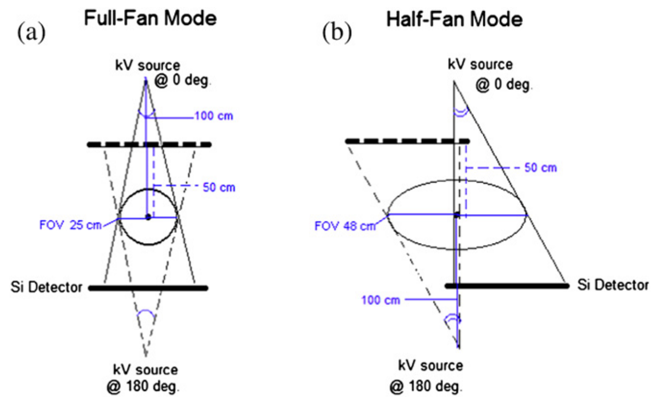

Fig. 2. Cone-beam CT imaging geometry: (a) full-fan mode, (b) half-fan mode.

Target localization

The intended study design was as follows: (*1*) to use CBCT as the gold standard for target localization and (*2*) to use single 40° arc DTS in either coronal or sagittal orientation as a CBCT replacement. The interfraction liver position reproducibility of daily treatment was evaluated retrospectively after all image data were collected. The image data sets of each modality were grouped and analyzed together. The coronal and sagittal DTS data sets were treated as independent modalities. Target positioning measured by each modality was blinded to the other modalities. Image registration was performed on imaging registration software supplied by the vendor (Offline Review, Varian Medical Systems Palo Alto, CA). Soft tissue–based alignment was performed for liver and tumor localization by aligning the reference 3D images (either reference CT or reference DTS) with the corresponding onboard images, *i.e.,* BH-CBCT with BH-CT, and BH-DTS with BH-RDTS. When tumor boundaries were distinguishable on some patients, both the tumor volume and the entire liver were used for soft tissue alignment. When tumor boundaries were not visible, the liver shape was used as a surrogate for soft tissue alignment. Because DTS is a relatively new imaging modality for radiation therapy, automatic registration algorithms for soft tissue target localization were not available for this study. For consistency, manual registration was performed for all imaging modalities. Target position variations were translated into couch shifts in the vertical, longitudinal, and lateral directions.

DTS yields 3D slice images with high in-plane resolution, although low out-of-plane or plane-to-plane (*i.e.,* in the direction perpendicular to the reconstruction planes) resolution (22, 25–27). For the coronal DTS, the out-of-plane direction is the couch vertical direction; for the sagittal DTS, the out-of-plane direction is the couch lateral direction. The accuracy of registration also included the comparison of the in-plane vs. out-of-plane directions.

Statistical analysis

All the registrations were performed by two independent reviewers. To assess the difference in target localization between the DTS and CBCT imaging techniques, we computed the mean, absolute mean, and standard deviation of the target positioning difference [*i.e.,* P(coronal-DTS) – P(CBCT) and P(Sagittal-DTS) – P(CBCT)] for each of the three couch directions. The results of the two reviewers were averaged to calculate the target positioning for each imaging technique. For this study, the CBCT-based soft tissue alignment was considered the gold standard. The two DTS

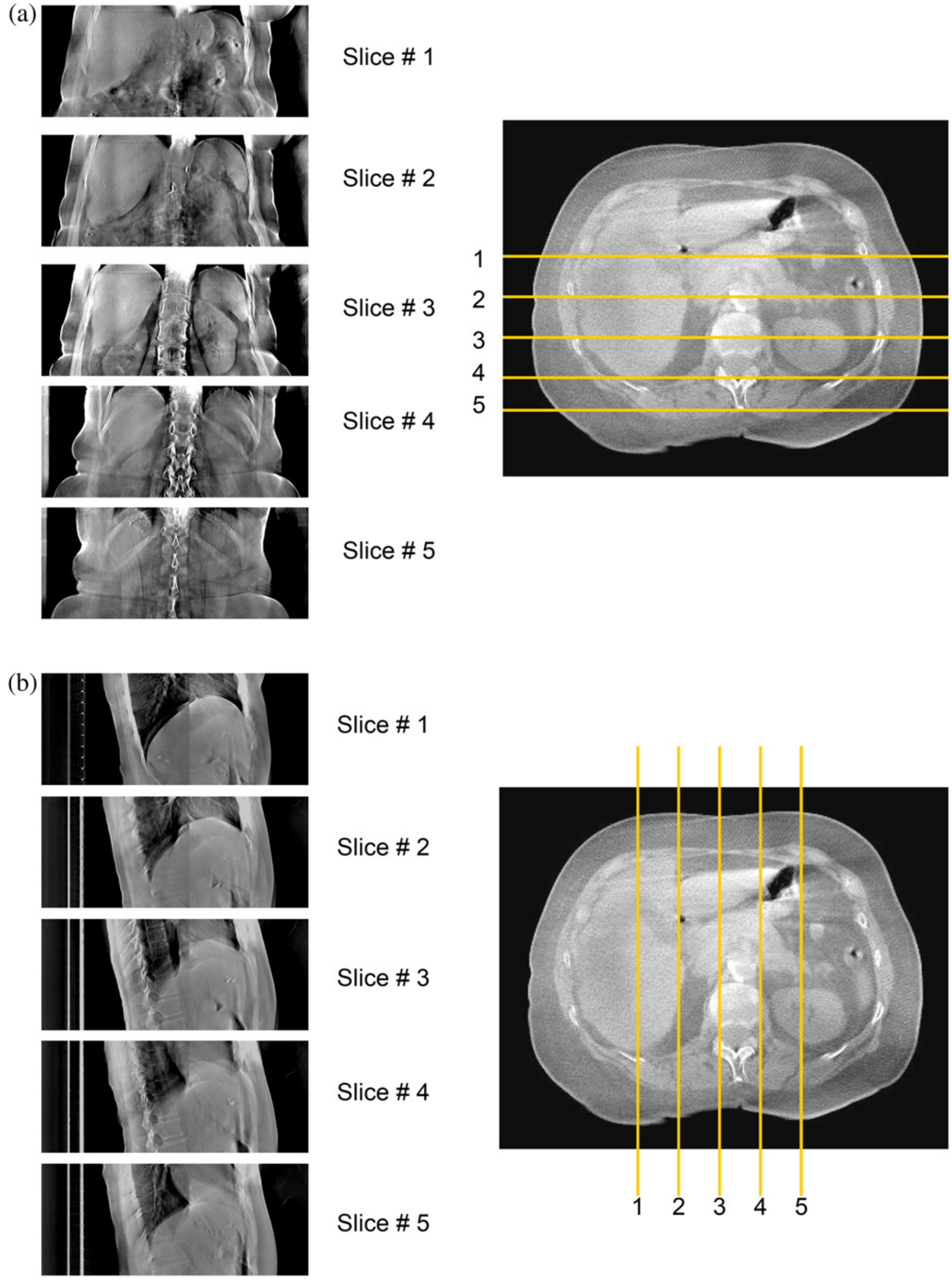

Fig. 3. Example images of the coronal (a) and sagittal (b) digital tomosynthesis (DTS) orientations used in this study. Each DTS reconstruction set is actually a stitched-together composite of two separate opposed DTS scans, reconstructed from subsets of half-fan (detector offset) cone-beam CT projection data. A true prospective DTS scan would only require a single scan orientation, because no half-fan detector offset would be implemented.

image sets were considered independent methods and were separately compared with the CBCT method.

In addition, the target localization agreement between the observers for each technique and the agreement between different techniques were analyzed. Pearson cross correlation coefficients were computed to evaluate the similarity and consistency.

RESULTS

DTS localization accuracy

Thirty-eight imaging fractions were studied for 14 patients. Table 1 shows the target localization accuracy of the two DTS methods, against the CBCT. The mean differences between the DTS methods and the CBCT method were <1 mm in all directions except in the lateral direction of the sagittal DTS (1.2 mm), indicating that the DTS methods were not biased. The absolute mean differences between the CBCT and DTS were in the range of 1.4–2.4 mm. The localization accuracy variations, indicated by standard deviation, were in the range of 2.1–3.5 mm.

Table 2 shows the Pearson correlation coefficients between the DTS and CBCT methods per individual couch direction. Overall, the coronal DTS showed better agreement

Table 1. Localization differences between CBCT and DTS

	CBCT−Coronal DTS			CBCT−Sagittal DTS		
	Lateral	Longitudinal	Vertical	Lateral	Longitudinal	Vertical
Absolute mean	1.4	1.9	2.2	2.4	2.2	2.4
Mean	−0.3	−0.3	0.9	1.2	0.4	−0.3
SD of mean	2.1	2.8	3.1	3.5	3.3	3.1

Abbreviations: CBCT = cone-beam CT; DTS = digital tomosynthesis.
All unit in millimeters.

with CBCT than the sagittal DTS. The agreement was in the range of 0.80–0.90 between the coronal-DTS and CBCT for the in-plane directions. The agreement was slightly lower, in the range of 0.72–0.88, between the sagittal-DTS and CBCT for the in-plane directions. The out-of-plane directions showed worse agreement compared with the in-plane directions. However, the agreement was still better for the coronal-DTS in the vertical direction than the moderate agreement achieved with sagittal-DTS in the lateral direction (the out-of-plane directions for the two DTS methods).

Interobserver variation

Table 3 and 4 show the target positioning between the two observers using the same technique. The mean difference of target localization was <1 mm except the lateral direction with Sagittal-DTS, which was 1.2 mm. The standard deviation of the interobserver variation was in the 1.5 mm range for the CBCT method and was approximately twice that (2.4–3.6 mm) for the DTS methods. The inter-observer agreement was in the range of 0.92–0.95 with the CBCT method, indicating almost perfect agreement. The interobserver agreement with coronal-DTS method was in the range of 0.72–0.78 for all directions, indicating that the agreement between the observers was not substantially worse in the out-of–plane dimension than it was for the other two high resolution dimensions. The interobserver agreement with the sagittal-DTS method, however, showed good agreement for the in-plane directions (vertical and longitudinal) but poor agreement in the out-of-plane direction (lateral). Hence, the out-of-plane blurring effect may have degraded the sagittal-DTS lateral registration consistency.

DISCUSSION

As a part of the initial investigation of DTS applications in target localization for radiation therapy treatment, this study evaluated the DTS imaging guidance for BH treatment. Overall, the mean difference between DTS and CBCT target localization performance found in this study was <1 mm, suggesting that the DTS method is unbiased relative to the CBCT method. Yet BH-DTS can be acquired with much less gantry rotation (<40°), which can be performed in one single breath-hold. Hence, the BH-DTS scan time is only roughly 10 s, compared with 3–4 min for BH-CBCT.

Interobserver variation

As stated previously, DTS yields 3D slice images with good in-plane resolution but lower plane-to-plane or out-of-plane (*i.e.,* in the direction perpendicular to the reconstruction planes) resolution. This may affect both the localization accuracy, defined as the difference between DTS and the CBCT results (mean and absolute mean differences), and the consistency, as indicated by the interobserver variation. The Pearson coefficient is more sensitive to direction shift but less sensitive to magnitude variations. For example, two observers could produce perfectly correlated measurements (*i.e.,* shift in same couch direction), but one observer could always underestimate the shift by 5 mm. However, if the two observers shift the couch in opposite direction, even by 1 mm in magnitude, the Pearson coefficients will be low. The quantitative analysis using mean and standard deviation statistics supplements the directional/trend indicator such as the Pearson correlation analysis. In this study, we found the mean differences between CBCT and DTS localizations were within 1 mm, indicating DTS is a nonbiased localization method. The standard deviations were in the range of 2.1–3.5 mm, with out-of-plane directions being slightly higher than in-plane directions. The interobserver variation was also larger with DTS methods (SD 2.4–3.6 mm) compared with CBCT methods (SD 1.4–1.7 mm). Furthermore, the CBCT-DTS agreement in the out-of-plane directions were worse than the in-plane directions, and the interobserver

Table 2. Pearson correlation between CBCT and DTS

	CBCT: Coronal DTS			CBCT: Sagittal DTS		
	Lateral	Longitudinal	Vertical*	Lateral*	Longitudinal	Vertical
Observer 1	0.90	0.82	*0.75*	*0.59*	0.78	0.88
Observer 2	0.80	0.88	*0.82*	*0.32*	0.72	0.72

Abbreviations: CBCT = cone-beam CT; DTS = digital tomosynthesis.
* Out-of-plane directions.

Table 3. Pearson correlation between observers

	Lateral	Longitudinal	Vertical
CBCT	0.92	0.94	0.95
Coronal DTS	0.72	0.78	*0.73**
Sagittal DTS	*0.26**	0.82	0.70

Abbreviations: CBCT = cone-beam CT; DTS = digital tomosynthesis.
* Out-of-plane directions.

agreement also showed worse results for the out-of-plane directions. This suggests that the out-of-plane DTS blurring affected the localization performance and the errors were random (*i.e.,* small mean difference but low correlation). Overall, the localization precision with DTS (95% confidence level in the –7 mm range) is larger than the interobserver variation using CBCT (95% confidence level in the 3–4 mm range) but comparable to the interobserver variation with DTS (95% confidence level also in the 4–7 mm range). As a result, it can be concluded that most of the DTS localization errors are random errors that might be improved by the future implementation of computer-aided localization algorithms. Recently, such algorithms have been under investigation to compensate for the reduced resolution in the out-of-plane direction and reduce the random errors (28). We have tested automatic DTS registration algorithms for bony anatomy and the results suggest that bony registration accuracy is equivalent in in-plane and out-of-plane directions (28). Further development of such algorithms for soft-tissue based registration has the potential to improve the localization accuracy reported in this study, with the hope that the DTS localization precision might ultimately approach the localization precision of CBCT.

Managing breath-hold variability

For tumors in the liver, reducing the treatment margin for organ motion due to breathing reduces the volume of normal tissues that are irradiated. The BH technique is effective in reducing organ motion and can be readily implemented in the clinic with a breathing monitoring device. However, even when patients are treated with the same reference BH window, variations still exist because of patient breathing habit change (*e.g.,* chest breathing vs. abdomen breathing) during the course of the treatment and other physiological changes that affects the breathing (20, 29). These factors are unforeseeable and may change the preset correlation between the external marker and internal anatomy during treatment simulation and the preset relative positions between the bony landmarks and the soft tissue target. With daily soft tissue based image-guidance, such as BH-CBCT and BH-DTS, the target position variation can be directly visualized and corrected.

Because of the differences in the distribution of BH segments over the total acquisition angle (as shown in Fig. 1b), the variations of BH levels manifest differently in images from different modalities. Figure 4 shows an example of this effect. Because the planning CT was acquired slice by slice with the couch moving longitudinally, each BH segment covers a subset of CT slices. The entire 3D volume is imaged during different BH segments, and these multiple BH segments are distributed in the superior to inferior direction. Therefore, variations of the BH levels would only manifest in the longitudinal direction; in some cases, the liver appears to have lost its surface continuity, as shown in Fig. 4a.

For CBCT, the couch is stationary, and the entire 3D anatomy is imaged by the cone-shaped beam. Each BH segment covers a subset of projection images or gantry rotations. Multiple BH segments occur at different gantry or projection angles. The variation in anatomy positions among different BH segments results in a blurred CBCT image after reconstruction, in all 3D planes, as shown with blurred liver boundaries and surgical clips in Fig. 4b. The DTS images usually only require a single BH and thus should not show any artifacts from such BH-level variations, as shown with crisp liver boundaries and surgical clips in Fig. 4c.

For a patient with large variability between BHs, multiple BH imaging may actually be preferred because it displays the average location of the target, the extent of the target position variation, or both. In this sense, CBCT is already an averaged imaging because of its use of multiple BH segments. Therefore, when large variability of BHs occurs, the CBCT images provide a blurred and averaged target volume and position. DTS, in contrast, is naturally acquired with a single BH and thus does not show the BH variability. However, in case of large BH-level variation, multiple single BH-DTS imaging is possible, given its fast acquisition and low dose compared with CBCT. In this sense, the multiple BH-DTS may also provide a complete picture of BH variability. Further, the BH-DTS images show a crisp (unlike the blurred CBCT) snapshot of the liver/target position under different BH levels or physical conditions, while providing the potential of quantitative correlation of external BH level variation to internal target position variation. Through multiple BH-

Table 4. Localization differences between observers

	CBCT			Coronal DTS			Sagittal DTS		
	Lateral	Longitudinal	Vertical	Lateral	Longitudinal	Vertical	Lateral	Longitudinal	Vertical
Mean	–0.1	0.1	–0.4	0.1	0.0	–0.3	1.2	–0.3	–0.7
SD	1.5	1.7	1.4	2.4	3.6	3.3	3.6	2.7	3.0

Abbreviations: CBCT = cone-beam CT; DTS = digital tomosynthesis.
All unit in millimeters.

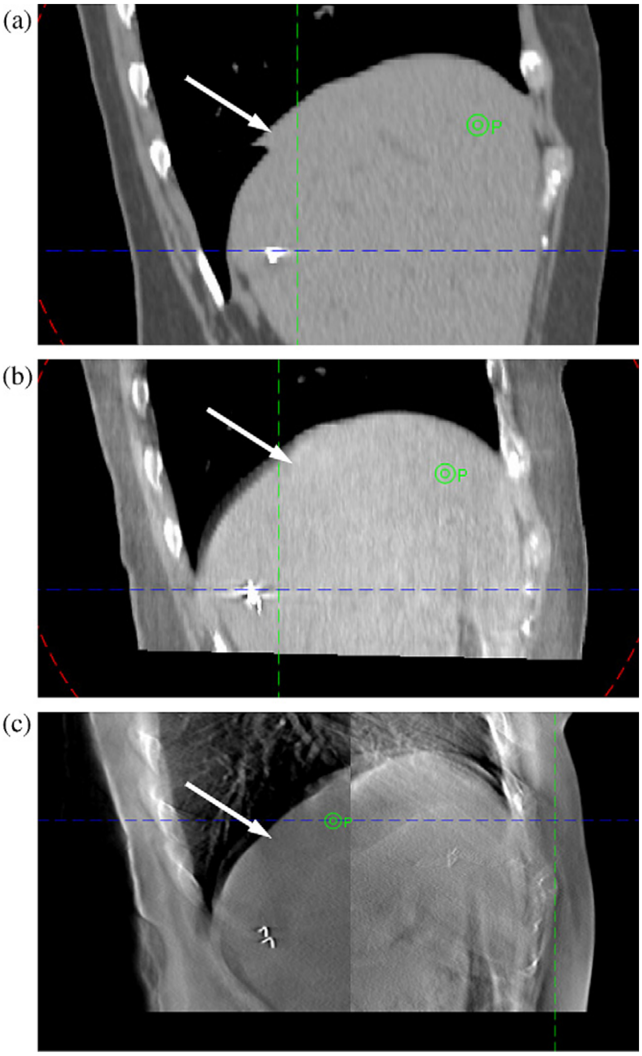

Fig. 4. Breath-hold variability artifacts for different imaging modalities: (a) CT, (b) cone-beam CT, and (c) digital tomosynthesis.

DTS imaging, the BH variation before each treatment fraction could be evaluated, and the BH threshold window and target position range could potentially be established and adjusted on a daily basis. This adaptive approach has the potential to improve BH treatment accuracy and may not be possible with BH-CBCT. In this regard, the development of automated DTS registration will be necessary to facilitate and expedite the clinical application of adaptive DTS-based onboard imaging guidance. Efforts are underway to develop algorithms that can perform both bony and soft tissue–based automatic registrations for this purpose.

It should be noted that the different presentation of BH-level variations may have had some impact on the target localization agreement between the DTS and CBCT methods. This BH-level variation effect was observed in this study but was not quantitatively analyzed because there were few cases with large apparent BH variations.

Future image quality improvements

The effect of out-of-plane anatomic structure blurring in DTS is well known because of incomplete projection data (22, 25–27). Attempts to improve the handling of out-of-plane detail in limited angle DTS scans are currently under investigation, including a promising technique that uses prior information to estimate optimally the out-of-plane anatomic information. The latest study by Ren *et al.* (30), using a deformable field method to generate limited scan angle 3D reconstructions, appears to be promising in this regard, because they have demonstrated the ability to reconstruct fully-3D CBCT-like volumes from limited angle DTS scans, using prior patient CT or CBCT data. However, more rigorous studies are necessary to investigate and quantify the inaccuracies induced by using prior images, especially when large changes in patient anatomy occur.

CONCLUSIONS

This study evaluated the localization accuracy and consistency using DTS (compared with CBCT as the gold standard) for BH treatment of liver cancer. The main advantage of DTS imaging is its fast acquisition within 1 BH (total imaging time of ~10 s) vs. multiple BH segments parsed over gantry rotations for BH-CBCT (total imaging time: 3–5 min), making it a potentially simple alternative to CBCT for onboard soft tissue imaging of the liver. The mean localization difference was <1 mm between the fast DTS techniques and the CBCT technique, and the standard deviations were in the range of 2.1–3.5 mm. The interobserver variation was also larger with DTS methods (SD 2.4–3.6 mm) compared with CBCT methods (SD 1.4–1.7 mm) because of the out-of-plane blurring that affects the consistency and the precision of manual localization using DTS. To make DTS a clinically applicable onboard imaging guidance option, future work should focus on automatic image registration specifically tailored for the DTS technique, with the goal of further improving the localization accuracy, and mitigating the impact of interobserver variability.

REFERENCES

1. Balter JM, Ten Haken RK, Lawrence TS, *et al*. Uncertainties in CT-based radiation therapy treatment planning associated with patient breathing. *Int J Radiat Oncol Biol Phys* 1996;36:167–174.
2. Berbeco RI, Nishioka S, Shirato H, *et al*. Residual motion of lung tumors in end-of-inhale respiratory gated radiotherapy based on external surrogates. *Med Phys* 2006;33:4149–4156.
3. Blackall JM, Ahmad S, Miquel ME, *et al*. MRI-based measurements of respiratory motion variability and assessment of imaging strategies for radiotherapy planning. *Phys Med Biol* 2006; 51:4147–4169.
4. Brandner ED, Wu A, Chen H, *et al*. Abdominal organ motion measured using 4D CT. *Int J Radiat Oncol Biol Phys* 2006; 65:554–560.

5. Rosu M, Dawson LA, Balter JM, *et al*. Alterations in normal liver doses due to organ motion. *Int J Radiat Oncol Biol Phys* 2003;57:1472–1479.
6. Balter JM, Brock KK, Litzenberg DW, *et al*. Daily targeting of intrahepatic tumors for radiotherapy. *Int J Radiat Oncol Biol Phys* 2002;52:266–271.
7. Dawson LA, Brock KK, Kazanjian S, *et al*. The reproducibility of organ position using active breathing control (ABC) during liver radiotherapy. *Int J Radiat Oncol Biol Phys* 2001;51: 1410–1421.
8. Herfarth KK, Debus J, Lohr F, *et al*. Extracranial stereotactic radiation therapy: Set-up accuracy of patients treated for liver metastases. *Int J Radiat Oncol Biol Phys* 2000;46:329–335.
9. Keall PJ, Mageras GS, Balter JM, *et al*. The management of respiratory motion in radiation oncology report of AAPM Task Group 76. *Med Phys* 2006;33:3874–3900.
10. Kim DJ, Murray BR, Halperin R, *et al*. Held-breath self-gating technique for radiotherapy of non-small-cell lung cancer: A feasibility study. *Int J Radiat Oncol Biol Phys* 2001;49:43–49.
11. Kimura T, Hirokawa Y, Murakami Y, *et al*. Reproducibility of organ position using voluntary breath-hold method with spirometer for extracranial stereotactic radiotherapy. *Int J Radiat Oncol Biol Phys* 2004;60:1307–1313.
12. Mageras GS, Yorke E. Deep inspiration breath hold and respiratory gating strategies for reducing organ motion in radiation treatment. *Semin Radiat Oncol* 2004;14:65–75.
13. Pattaranutaporn P, Chansilpa Y, Ieumwananonthachai N, *et al*. Three-dimensional conformal radiation therapy and periodic irradiation with the deep inspiration breath-hold technique for hepatocellular carcinoma. *J Med Assoc Thai* 2001;84:1692–1700.
14. Wong JW, Sharpe MB, Jaffray DA, *et al*. The use of active breathing control (ABC) to reduce margin for breathing motion. *Int J Radiat Oncol Biol Phys* 1999;44:911–919.
15. Yokokawa T, Shintani H. Development of picture and voice gated intermittent irradiation system connected without linear accelerator for voluntary breath-hold synchronized with respiration. *Nippon Igaku Hoshasen Gakkai Zasshi* 2002;62:290–291.
16. Yoshitake T, Nakamura K, Shioyama Y, *et al*. Breath-hold monitoring and visual feedback for radiotherapy using a charge-coupled device camera and a head-mounted display: System development and feasibility. *Radiat Med* 2008;26:50–55.
17. Dawson LA, Eccles C, Craig T. Individualized image guided iso-NTCP based liver cancer SBRT. *Acta Oncol* 2006;45: 856–864.
18. Eccles C, Brock KK, Bissonnette JP, *et al*. Reproducibility of liver position using active breathing coordinator for liver cancer radiotherapy. *Int J Radiat Oncol Biol Phys* 2006;64:751–759.
19. Dawson LA, Eccles C, Bissonnette JP, *et al*. Accuracy of daily image guidance for hypofractionated liver radiotherapy with active breathing control. *Int J Radiat Oncol Biol Phys* 2005;62: 1247–1252.
20. Hawkins MA, Brock KK, Eccles C, *et al*. Assessment of residual error in liver position using kV cone-beam computed tomography for liver cancer high-precision radiation therapy. *Int J Radiat Oncol Biol Phys* 2006;66:610–619.
21. Thompson BP, Hugo GD. Quality and accuracy of cone beam computed tomography gated by active breathing control. *Med Phys* 2008;35:5595–5608.
22. Godfrey DJ, Yin FF, Oldham M, *et al*. Digital tomosynthesis with an on-board kilovoltage imaging device. *Int J Radiat Oncol Biol Phys* 2006;65:8–15.
23. Wu QJ, Godfrey DJ, Wang Z, *et al*. On-board patient positioning for head-and-neck IMRT: Comparing digital tomosynthesis to kilovoltage radiography and cone-beam computed tomography. *Int J Radiat Oncol Biol Phys* 2007; 69:598–606.
24. Yoo S, Wu QJ, Godfrey D, *et al*. Clinical evaluation of positioning verification using digital tomosynthesis and bony anatomy and soft tissues for prostate image-guided radiotherapy. *Int J Radiat Oncol Biol Phys* 2009;73:296–305.
25. Badea C, Kolitsi Z, Pallikarakis N. A wavelet-based method for removal of out-of-plane structures in digital tomosynthesis. *Comput Med Imaging Graph* 1998;22:309–315.
26. Badea C, Kolitsi Z, Pallikarakis N. Image quality in extended arc filtered digital tomosynthesis. *Acta Radiol* 2001;42: 244–248.
27. Kolitsi Z, Panayiotakis G, Pallikarakis N. A method for selective removal of out-of-plane structures in digital tomosynthesis. *Med Phys* 1993;20:47–50.
28. Ren L, Godfrey DJ, Yan H, *et al*. Automatic registration between reference and on-board digital tomosynthesis images for positioning verification. *Med Phys* 2008;35:664–672.
29. Hansen AT, Petersen JB, Hoyer M. Internal movement, set-up accuracy and margins for stereotactic body radiotherapy using a stereotactic body frame. *Acta Oncol* 2006;45:948–952.
30. Ren L, Zhang J, Thongphiew D, *et al*. A novel digital tomosynthesis (DTS) reconstruction method using a deformation field map. *Med Phys* 2008;35:3110–3115.